Hybrid-III 5th Female Response and Kinematics in Frontal Impacts Using Vehicle Seats and Restraints Designed for Alternative Seating Positions

Rachel Newman, Jeesoo Shin, Bronislaw D. Gepner, Neal R. Morgan, Yongtae Kim, Sung Rae Kim, Jason R. Kerrigan

Abstract Non-traditional seating postures will challenge traditional occupant protection paradigms. The goal of this research was to evaluate restraint effectiveness by measuring how three different restraint configurations influenced Hybrid-III 5th female (HIII-5F) response in frontal sled tests with a vehicle seat. The seat was positioned in the rearmost seat track position, reclined 40° from vertical, incorporated a seat-integrated-belt (BIS), and had a leg rest that elevated the feet off the floor. Restraint configurations incorporated a: (1) seat cushion airbag (SCAB), large passenger airbag (PAB), and shoulder belt pretensioner (SB P/T); (2) SCAB, PAB, SB P/T, and anchor pretensioner (A P/T); (3) PAB, SB P/T, and A P/T. While each configuration uniquely affected HIII-5F kinematics, the HIII-5F submarined only in configuration #3, suggesting the SCAB had the biggest influence on submarining outcome. The vehicle seat allowed for more pelvis downward excursion than has been observed in previous studies on reclined occupants in simplified semi-rigid seats. Adding the A P/T in configuration #2 did not substantially improve predicted injury risk compared to configuration #1. Additional investigations with vehicle seats are necessary to determine if the same pelvis excursion and restraint configuration sensitivities exists for human occupants, and small-sized females, in particular.

Keywords Alternative seating positions, HIII-5F, seat cushion airbag, submarining, vehicle seat

I. INTRODUCTION

Promises of highly autonomous vehicles (HAVs) are challenging today's perspective of a vehicle's interior and how occupants might be seated within it. Development of these systems has allowed occupants to envision a landscape in which they can participate in extracurricular activities and sit in non-traditional postures [1, 2]. Although the promise of HAVs has yet to come to fruition, the concept of vehicles allowing for alternative seating positions is already being implemented for passengers other than the driver [3].

Vehicles with seats that allow occupants to sit in reclined positions are of particular interest to consumers because they allow for relaxation and comfort [1]. Real-world crash data has demonstrated that occupants in recline, when compared to those seated upright, have a higher risk of fatality and are more prone to injury at a given injury severity level [3–5]. Distance of an occupant from the knee bolster, a parameter expected to increase with reclined seating, also contributes to increased risk of injury [6–9]. Submarining is one of the most highly anticipated injury mechanisms for reclined occupants, with vulnerable occupants like small females predicted to be at greater risk [7, 9]. Submarining is the phenomenon in which the lap belt loses engagement with the pelvis and causes load initially applied to the pelvis to be transferred to the abdomen [10–14]. Abdominal loading causes injury to the internal organs, which are often assigned to AIS3+ injuries or higher [10–12] and in some cases can lead to fatality.

Although research has been performed to understand kinematics and injury response of occupants in recline, most experimental studies have been conducted in simplified environments, using a semi-rigid seat to replicate the angular stiffness of a real-vehicle seat pan [14–21]. However, simulations suggest that the semi-rigid seat allows for less downward pelvis excursion and less risk for submarining than an original equipment manufacturer (OEM) vehicle seat [6].

R. Newman (e-mail: rmn8ba@virginia.edu; tel: +1-434-297-8036) is a PhD student in Mechanical and Aerospace Engineering, J. Shin is a Research Engineer, B. Gepner is a Senior Scientist, N. Morgan is a Postdoctoral Research Associate, and J. Kerrigan is an Associate Professor of Mechanical and Aerospace Engineering, all at the University of Virginia Center for Applied Biomechanics, Charlottesville, Virginia, USA. Y. Kim and S. Kim are Senior Research Engineers at Hyundai Motor Company, Hwaseong, South Korea.

Further, these simplified environments are limited in their ability to translate their results to real-world vehicle structures and restraints, which may prove to be crucial in protecting occupants in recline. Research evaluating effective restraints for reclined occupants has largely limited its focus to belt pretensioners and load limiters. While these counter measures have proven to be effective in simplified environments, they represent just some of the countermeasures that might exist in a real-vehicle environment. To our knowledge, traditional structures like frontal airbags have yet to be evaluated experimentally in reclined postures, although they have been included in some computational work [22, 23]. Computationally, for reclined occupants, there has been investigation into the significance of knee bolster location and occupant knee bolster interaction [6–9], but translation of this into experimental studies has been limited in simplified environments [20, 21, 23].

Not only is there a need, experimentally, to evaluate the effectiveness of traditional restraints like frontal airbags and knee bolster positions, there is also a need to evaluate seat-integrated restraints that may be incorporated into future vehicles. Anticipated seat-integrated countermeasures include seat-integrated belts (BIS) [22, 24] and seat cushion airbags (SCAB). The BIS is expected to help improve belt fit, torso restraint, and head kinematics by reducing space between the shoulder belt and torso introduced by an occupant sitting in a non-traditional posture [2, 17, 25, 26]. The SCAB, sometimes referred to as a pelvis restraint cushion (PRC), has been shown to reduce forward and downward motion of the pelvis [2, 22, 27], kinematics predicted to be crucial in preventing submarining [6, 23]. In a real-vehicle environment, where the seat, in comparison to the semi-rigid seat, is expected to allow for more pelvis downward displacement and subsequent seat deformation, the SCAB may prove to be especially valuable in properly restraining and protecting the occupant [22, 23, 28].

There is a demonstrated need to evaluate the effectiveness of countermeasures in a real-vehicle environment, especially for anthropometries most at risk of submarining, such as small females. The goal of this research was to evaluate restraint effectiveness by measuring how three different restraint configurations influenced Hybrid-III 5th female (HIII-5F) response and kinematics in a crash environment with a vehicle seat designed for alternative seating positions.

II. METHODS

A reverse acceleration sled system (1.4 MN ServoSled®, Seattle Safety, Auburn, WA, USA) was used to perform three frontal impact, 38.8 g, 56 km/h sled tests (Fig. A1) with the Hybrid-III 5th female (HIII-5F). A global (sled) coordinate system (CS) was defined using SAE J211 specifications [29], with the +X axis pointing forward, +Y axis pointing outboard, and +Z axis pointing down. The origin was defined as the back right corner of the sled.

Test Matrix

The restraints included in this study were a dual-stage large passenger airbag (PAB), shoulder-belt retractor pretensioner (SB P/T), anchor pretensioner (A P/T), and seat cushion airbag (SCAB). Three different restraint configurations were tested. One test was performed for each restraint configuration (Table I). Configuration #1 used the SB P/T, PAB, and SCAB. Configuration #2 used the SB P/T, A P/T, PAB, and SCAB. Configuration #3 used the SB P/T, A P/T, and PAB.

TABLE I
TEST MATRIX AND ASSOCIATED RESTRAINT CONFIGURATIONS

		Restraint Configuration/ Test Number		
		Configuration #1 / S0902	Configuration #2 / S0903	Configuration #3 / S0904
Restraints	SB P/T	✓	✓	✓
	PAB	✓	✓	✓
	SCAB	✓	✓	
	A P/T		✓	✓

Test Environment

For each test, the sled was equipped with a body in white vehicle buck, which contained a steel instrument panel (IP), full frontal windshield, and passenger-side vehicle seat. The buck's passenger-side b-pillar was removed for added visibility of the occupant. A new seat was installed for each test. Foam was attached to the underside of the steel IP to act as a padded knee bolster. Unlike traditional vehicle seats, the seat used for this study was designed with a BIS and leg rest. Recline angle, seat travel, seat cushion height, seat cushion tilt angle, leg rest support angle and head rest position were all adjustable features of the seat. The seat was adjusted to the same initial orientation for each test.

The sled was also equipped with eight onboard high-speed video cameras operating at 1000 Hz. Two cameras were mounted atop "outriggers" attached to the sled to provide comprehensive, horizontally level, passenger and driver-side views of occupant kinematics relative to the entire buck (Fig. A2). One camera was mounted obliquely to the passenger-side outrigger to provide a passenger-side oblique view of the HIII-5F. Four cameras were mounted to various structures of the buck to capture overhead, overhead oblique, shoulder-belt retractor, and driver-side pelvis views throughout each test. One camera was mounted to the driver-side of the IP to capture driver-side oblique views of each test.

Restraints and Trigger Timing

The HIII-5F was restrained by a seat-integrated three-point BIS. The shoulder belt retractor was mounted to the seatback frame. The anchor and buckle were fixed to the outboard and inboard sides of the seat pan frame, respectively. The shoulder-belt retractor was equipped with a shoulder-belt load limiter of 3.5 kN and a SB P/T, which fired 12 ms after time zero. The PAB was installed inside the IP. The top of the IP had an opening for the PAB to allow for unobstructed deployment. The PAB was dual-stage and triggered at 12 and 16 ms. The SB P/T and PAB, along with their firing times, were used in all three restraint configurations.

An A P/T was used in restraint configurations #2 and #3. The A P/T was triggered at 19 ms. The seat cushion airbag (SCAB) was used in restraint configurations #1 and #2. The SCAB was attached to the seat pan frame and resided in between the seat pan frame and the seat pan cushion. The SCAB was triggered to deploy at 12 ms.

Seat Positioning

The seat was adjusted to the same initial orientation for each test. Seat travel was positioned in the most posterior position along the tracks, the seat back was reclined 40° from vertical, the seat cushion was tilted to the upmost setting, and the leg rest was lifted to the upmost position, so the feet were elevated off the floor (Fig. A3). In this orientation, seat cushion tilt and leg rest angle were 23° and 22.6° from the horizontal, respectively. Seat back recline angle was measured via the headrest poles before the head rest was lowered into position. The headrest was positioned in the lowest and forwardmost setting.

HIII-5F Positioning

The HIII-5F was centered on the seat and adjusted such that the anthropomorphic test device (ATD) was free of roll or yaw. Positioning and measurement targets were defined for the HIII-5F H-point position, pelvis angle, head CG position, head angle, knee position, knee lateral to lateral breadth, torso angle, heel lateral to lateral breadth, chest to IP distance, and head to windshield distance (Fig. A4). First, the HIII-5F was adjusted until the H-point position matched its positioning target. From this position, the torso was rested against the seatback and the arms were left to lay naturally within the seatback. The HIII-5F was then iteratively aligned to match the remainder of the positioning and measurement targets. An acromion tool for the HIII-5F was developed based on the methods described in Shin *et al.* [19]. The acromion tool and H-point were necessary for measurement of the torso angle in the sagittal plane.

Belt Positioning

Half-width lines were drawn on the belt every 1 cm and full-width lines were drawn on the belt every 5 cm at the anchor, latch plate, and shoulder belt retractor. Once the seat and HIII-5F were positioned, the belt was buckled over the ATD. The webbing length in the shoulder retractor was measured. The lap belt was routed as low as possible without roping/folding. The shoulder-belt was routed over the middle of the sternum and then iteratively adjusted to match measurement targets for the shoulder-belt relative to the HIII-5F chin and lap.

Buck and HIII-5F Instrumentation

Uniaxial belt gauge load cells (Seat belt load cell, MESSRING Systembau MSG GmbH, Krailling, Germany) were installed on the shoulder-belt and lap-belt. The shoulder-belt gauge was placed 150 mm below the BIS D-ring, and the lap-belt gauge was placed as close to the seat as possible without contacting the seat cushion. Tests performed in configurations #2 and #3 that used an A P/T were only able to use the shoulder-belt gauge as there was no space for the lap-belt gauge.

The HIII-5F was equipped with head accelerometers and angular rate sensors, an upper neck load cell, chest accelerometers, a chest deflection transducer, a lumbar spine load cell, pelvis accelerometers and angular rate sensors, anterior superior iliac spine (ASIS) load cells, and single axis femur load cells. The HIII-5F and the locations of its instrumentation are specified by the HIII-5F manual and drawing package [30, 31]. All instrumentation were in accordance with SAE J211 polarity definitions [29]. The HIII-5F was certified prior to testing.

VICON Motion Tracking

A 1000-Hz Vicon MX^{TM} 3D camera-based motion capture system (Vicon MX^{TM}, VICON, Centennial, CO, USA) and retroreflective spherical markers were used to track occupant, belt, seat frame, and buck kinematics. Surface markers were attached to the seat frame, belt webbing and the HIII-5F. Marker clusters, which contained a minimum of four retroreflective spherical markers, were attached by rigid fixation to the buck and the HIII-5F head, spine, and pelvis.

The marker array affixed to the pelvis consisted of two four-marker clusters protruding posteriorly out of the HIII-5F. Careful design was involved to ensure the pelvis mount protruded posteriorly between the HIII-5F pelvis mold and chest jacket without interfering with these features of the ATD. Parts of the seatback cushion were cut away to enable visibility of the motion tracking marker clusters fixed to the HIII-5F pelvis. The suspension springs in the seatback also had to be removed to allow for VICON visibility of motion tracking marker clusters fixed to the pelvis. Removal of these seatback components did not impact the natural seated position of the HIII-5F.

Kinematics Data Analysis

The position and orientation of each anatomical structure with a rigidly attached Vicon marker clusters was calculated relative to the defined global CS. Collection of rigidly fixated Vicon marker cluster data along with measurements of the marker cluster locations relative to each HIII-5F anatomical structure allowed for the use of coordinate transformations to determine position and orientation of each HIII-5F anatomical structure relative to the buck [32].

Local accelerations and angular rates of the head and pelvis were calculated using raw accelerometer and angular rate data along with measurements of the sensors' positions relative to the head and pelvis CGs [32]. The local anatomical CS definitions are shown in Fig. A4.

III. RESULTS

The seated anthropometric measurements (Fig. A5) for each test can be found in Table II.

TABLE II
SEATED ANTHROPOMETRIC MEASUREMENTS FROM EACH SLED TEST

	S0902	**S0903**	**S0904**
Pelvis angle	40.1°	40.5°	38.75°
Torso angle	39°	41°	40.5°
Head angle	18.6°	18.5°	18.2°
Chest to IP	940 mm	950 mm	945 mm
Knee lateral to lateral breadth	320 mm	325 mm	320 mm
Head to Windshield distance	1100 mm	1095 mm	1095 mm
Heel lateral to lateral breadth	185 mm	190 mm	185 mm

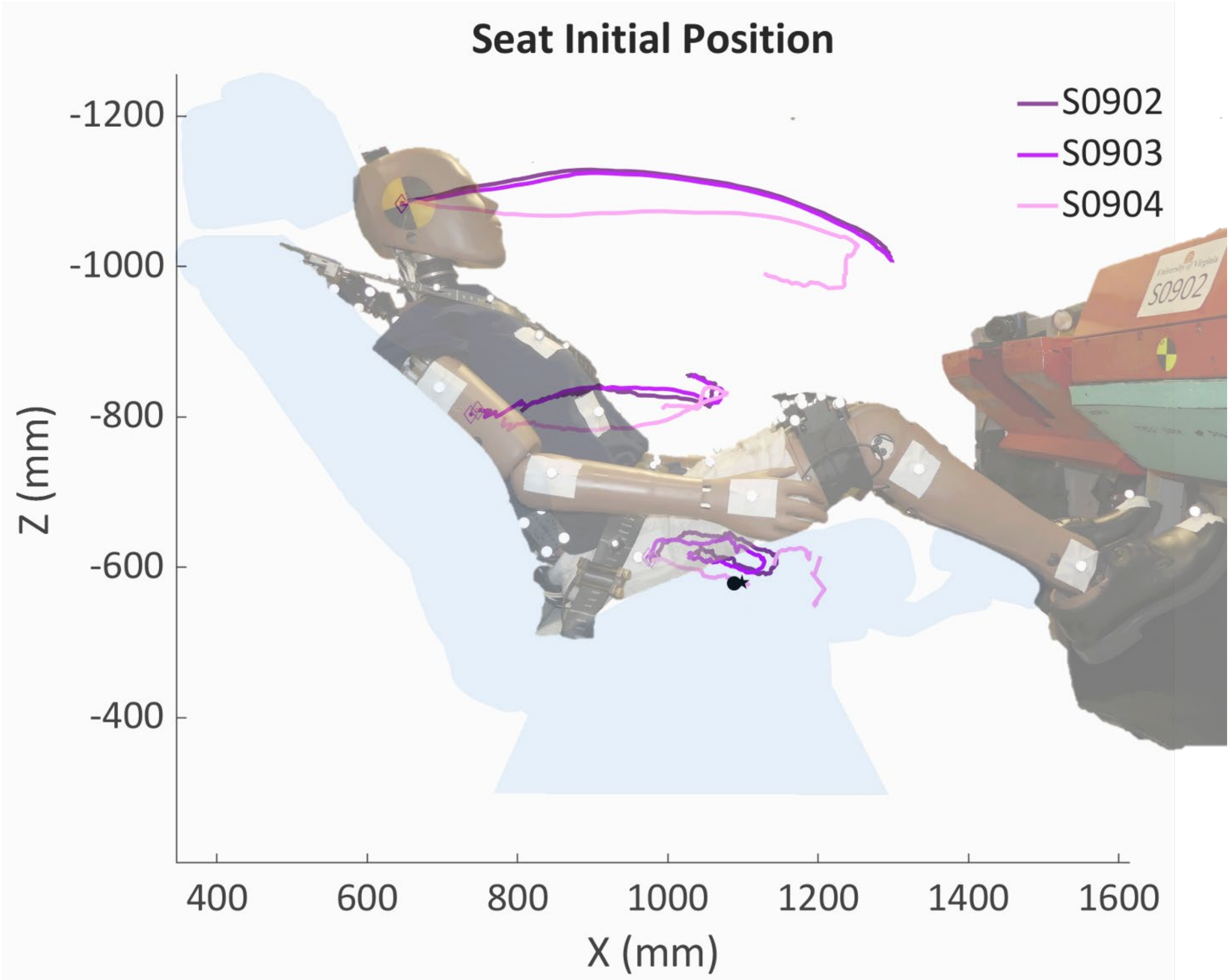

Fig. 1. Head, spine, and pelvis trajectories relative to the initial position of the seat, HIII-5F, and IP from 0-140 ms. Submarining in S0904 on the buckle-side is denoted by a circle. Submarining in S0904 on the anchor side is denoted by a star. For S0902 and S0903, VICON visibility of the head marker cluster was lost at 108 ms. For S0904, Vicon visibility of the pelvis marker cluster was obstructed from 63-84 ms and after 114 ms.

Occupant Kinematics

Trajectories of the head, spine block, and pelvis were plotted relative to the initial position of the vehicle seat and IP (Fig. 1). Tests run in configurations #1 and #2 had similar trajectories of the head, spine and pelvis while the test performed in configuration #3, which did not include a seat cushion airbag (SCAB), had noticeably different trajectories of the head, spine and pelvis.

Submarining occurred only in configuration #3 at 57 and 60 ms on the left (buckle/inboard) and right (anchor/outboard) sides, respectively. Minimal downward translation and approximately 7.3°-9.8° of initial rearward rotation of the pelvis were observed in the tests with the SCAB (Fig. 2). Maximum rearward rotation of the pelvis occurred between 35-36 ms for restraint configurations #1 and #2. Exclusion of the SCAB in configuration #3 led to initial downward translation of the pelvis into the seat and delayed its rearward rotation. In configuration #3, the pelvis measured 11° of rearward rotation at approximately 74 ms. After submarining, between 63-84 ms, VICON visibility of the pelvis marker clusters was lost in restraint configuration #3. At least 62 mm of downward displacement of the pelvis was observed in restraint configuration #3, though it is suspected more downward displacement occurred after visibility of the pelvis marker clusters was obstructed (Fig. 3). Peak forward pelvis excursion was 165, 155, and 227 mm and occurred at 86, 87, and 91 ms for restraint configurations #1, #2, and #3, respectively (Fig. B7). For all three restraint configurations, at peak forward pelvis excursion, the pelvis rotation had returned approximately to its initial orientation.

In the absence of the SCAB, there was less forward and upwards displacement of the head. Furthermore, forward rotation of the head was delayed and occurred at a higher angular rate in configuration #3 relative to configurations #1 and #2 (Fig. B3). The first contact of the head with the PAB occurred at 89 ms in each test. Peak measured forward head excursion was 657, 652, and 601 mm for restraint configurations #1, #2, and #3, respectively (Fig. B1).

The HIII-5F spine experienced more downward displacement in configuration #3 compared to the tests run in configurations #1 and #2 (Fig. B5). The HIII-5F experienced less flexion of the spine in restraint configuration #3 compared to configurations #1 and #2 (Fig. B6). Peaks in chest displacement at approximately 25 ms are caused by the shoulder belt pretensioner. Peak chest displacement was largest, 16.5 mm, in restraint configuration #3 when the HIII-5F submarined. (Fig. D10)

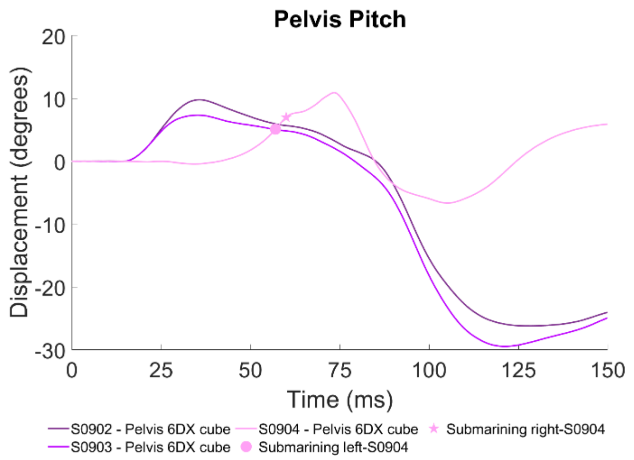

Fig. 2. Pelvis rotation in the sagittal plane relative to the local pelvis CS. Positive displacement corresponds with rearward rotation of the pelvis. Submarining in S0904 is marked on the pelvis trajectory.

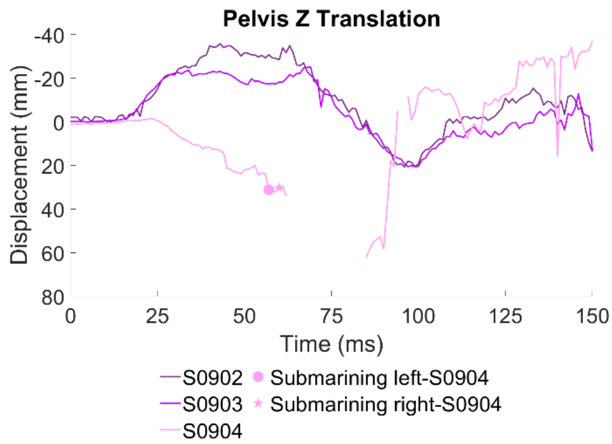

Fig. 3. Pelvis z-displacement time history relative to the global CS. Negative displacement corresponds with upwards excursion of the pelvis. Submarining in S0904 is marked on the pelvis trajectory. Submarining on the buckle-side is denoted by a circle. Submarining on the anchor side is denoted by a star. After submarining, between 63-84 ms, VICON visibility of the pelvis marker clusters was lost.

Belt Performance

Belt performance measurements, measured at the shoulder-belt retractor can be found in TABLE CI. Shoulder belt pay-out was largest in the test run in restraint configuration #3 where the HIII-5F submarined.

Loads and Sensor Measurements

Lap belt force could only be measured in restraint configuration #1 without the A P/T. Peak lap belt force was 6.6 kN and occurred just before the pelvis reached peak forward excursion (Fig. 4). An initial spike in shoulder belt force was measured at 16 ms when the SB P/T fired. Shoulder belt forces plateaued around 3.5 kN across all three restraint configurations (Fig. 5). For restraint configurations #1 and #2, chest accelerations and displacements were similar (Fig. D7-D10). Maximum chest displacements were 13.0, 12.3, and 16.5 mm for restraint configurations #1, #2, and #3, respectively.

Left and right ASIS force peaked between 3-4 kN in tests that included a SCAB (Fig. 6, Fig. 7). The peak ASIS force on both the left and right ASIS was largest when both the A P/T and SCAB were included in the restraint environment. Left and right ASIS forces reached peaks of approximately 1.5 kN in restraint configuration #3. Drops in left and right ASIS load cell forces aligned with buckle and anchor side submarining event timing.

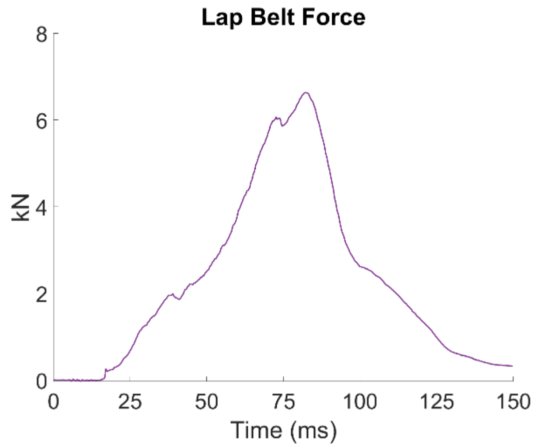

Fig. 4. Lap belt force in restraint configuration #1 (S0902).

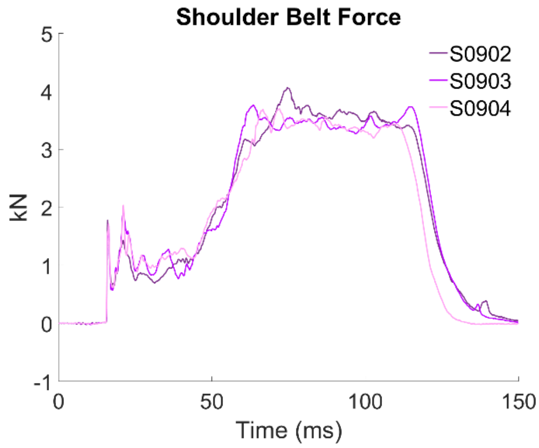

Fig. 5. Shoulder belt forces in each restraint configuration.

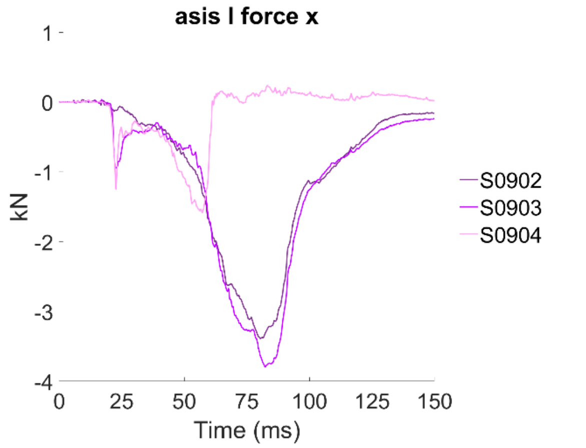

Fig. 6. Left ASIS force measured at the left iliac wing load cell along its anterior-posterior axis.

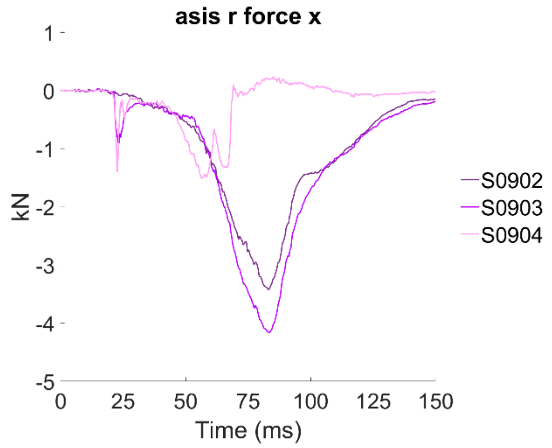

Fig. 7. Right ASIS force measured at the right iliac wing load cell along its anterior-posterior axis.

Femur forces peaked at approximately 2 kN in configurations #1 and #2. For configuration #3, left and right femur forces peaked between 2.7-3.1 kN (Fig. D11, Fig. D12). Positive femur forces correspond with tension. The HIII-5F knees never contacted the foam underneath the IP in any of the three tests performed, which caused tensile, rather than compressive, forces to be measured at the femurs. Although the knees never contacted the foam beneath the IP, the HIII-5F feet interacted with the foam underneath the IP in each test.

Lumbar forces and moments were comparable in tests run in restraint configurations #1 and #2 (Fig. 8-10). Between 10-20 ms after the SCAB was triggered to inflate, 1.7 kN of lumbar spine compression and approximately 0.6 kN of positive anterior-posterior shear loading in the spine block was observed. In restraint configurations #1 and #2, lumbar spine compression never exceeded the peak compression force experienced immediately after SCAB deployment (Fig. 8). Lumbar spine compression forces were reduced in restraint configurations #1 and #2 compared with configuration #3 (Fig. 9). Deployment of the SCAB also produced an initial peak, between 30-40 Nm, in flexion bending moment applied to the lumbar spine (Fig. 10). Tests run with a SCAB saw maximum lumbar flexion bending moments between 220-255 Nm (Fig. 10).

In the absence of a SCAB, initial lumbar spine compression was not observed. Upon submarining in restraint configuration #3, the lumbar spine was put under a peak compressive force of approximately 5 kN, and positive anterior shear force increased as the torso and spine began bearing load initially applied to the ASIS load cells. Lumbar spine compression forces were highest in restraint configuration #3 after the HIII-5F submarined. Unlike configurations #1 and #2, initial positive peaks in lumbar spine flexion bending moment were not observed for configuration #3. However, submarining in restraint configuration #3 increased the extension bending moment measured at the lumbar spine load cell.

Head (Fig. D3-D6) and upper neck (Fig. D13-D15) responses were comparable across all three tests until approximately 57 ms, when the HIII-5F submarined in restraint configuration #3. After 57 ms, head and neck responses in restraint configuration #3 deviated from those in restraint configurations #1 and #2. Most notably, tests performed in restraint configurations #1 and #2 only ever measured tensile forces at the upper neck load cell while compression in the upper neck was measured after HIII-5F submarining in restraint configuration #3 (Fig. D14). Extension and flexion bending moment were observed at the upper neck in restraint configurations #1 and #2 whereas, minimal extension bending moment was measured at the upper neck load cell in the test run in restraint configuration #3 (Fig. D15).

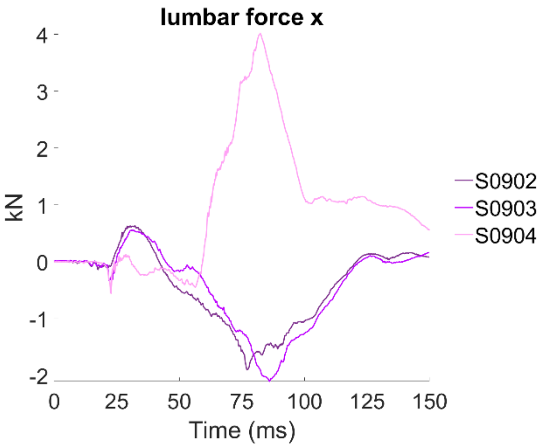

Fig. 8. Lumbar spine anterior-posterior shear force. Positive forces can be described by rearward motion of the chest and forward motion of the pelvis.

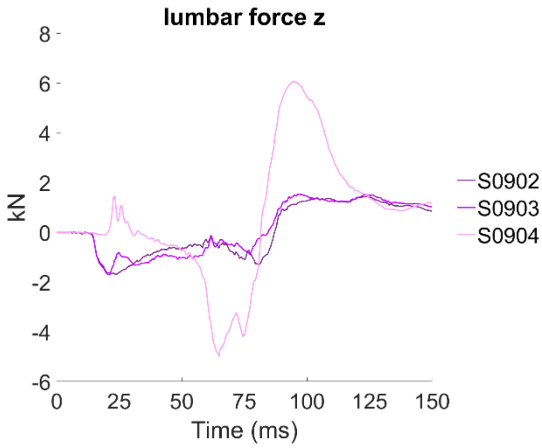

Fig. 9. Lumbar spine axial loads. Compression is negative. Tension is positive.

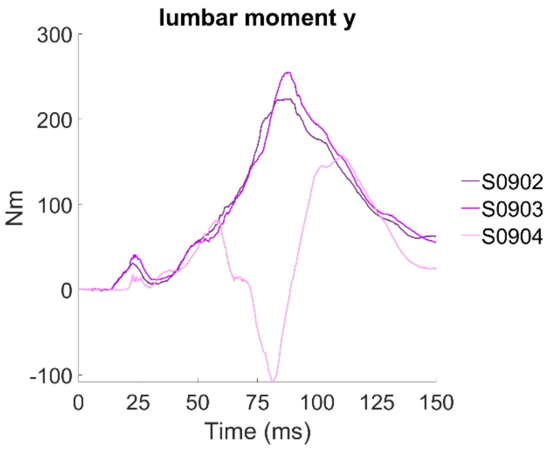

Fig. 10. Lumbar spine flexion-extension bending moment. Flexion bending moment is positive (sternum rotating towards the front of the legs). Extension bending moment is negative (sternum rotating away from the front of the legs).

IV. DISCUSSION

This study allowed us to isolate the effect of individual restraints on the kinematic and kinetic response of a HIII-5F seated (1) in a real-vehicle seat, (2) in a reclined posture, (3) with feet elevated off the floor through means of a leg rest and, (4) further away from the instrument panel than is traditionally allowed for. Across the three restraint configurations tested, the biggest differences in HIII-5F kinematic and kinetic response were observed in restraint configuration #3, the only configuration that did not include a SCAB.

Effect of SCAB on Occupant Response

The seat cushion airbag (SCAB) introduced an upwards force into the crash environment that was applied to the HIII-5F at the pelvis. The upwards force presented by the SCAB and applied to the HIII-5F pelvis was partially counteracted by the combined inertial and lap belt forces in a frontal crash that induce forward and downward motion of an occupant [23]. For tests performed with a SCAB, the HIII-5F had an initial upward and forward motion (Fig. 1). Pelvis vertical displacement following SCAB deployment in a frontal crash impact aligns with what has been seen computationally with human body models (HBMs) of different anthropometries [22]. After inflation of the SCAB, the SCAB's pressure and consequently, applied force, were reduced. While the impact of the SCAB diminished, inertial and lap belt forces remained, permitting downward displacement of the HIII-5F prior to rebound. The upwards force applied to the HIII-5F because of SCAB deployment caused an initial rearward rotation of the pelvis. Following peak rearward rotation, the pelvis rotated forward. Pelvis forward rotation was most likely a consequence of the persistent downward force and restraint applied to the lap via the lap belt along with the inertial forces of the crash causing the HIII-5F torso to flex forward and the shoulder belt to pay out. Since lumbar spine injury risk criterion does not exist, there is no way to interpret the lumbar spine forces measured by the HIII-5F. What can be concluded is that, compared with restraint configuration #3, inclusion of a SCAB in restraint environments #1 and #2 reduced the positive anterior-posterior shear, compressive, and tensile forces and reduced the extension bending moments measured at the lumbar spine load cell of the HIII-5F.

Previous upright frontal impact tests with female post-mortem human subjects (PMHS) [27] found that a SCAB did not have much impact on peak vertical upward pelvis motion. Contrary to Shaw et al. [27], the current study found large differences between peak pelvis vertical motion of the HIII-5F when the SCAB was not present (Fig. 1). In the absence of the SCAB, the typical forward and downward occupant motion expected in frontal crash environments was observed. The downward translation of the HIII-5F pelvis into the seat was absorbed by the seat pan. In the absence of the SCAB in configuration #3, the HIII-5F experienced the largest downward displacement of the pelvis observed in this study. This demonstrates, in agreement with previous work [23], that the SCAB reduces downward excursion of the pelvis. Rearward rotation of the pelvis occurred much later in the crash event when compared to restraint configurations #1 and #2. We suspect rearward rotation began when the pelvis either bottomed out the seat pan suspension springs or translated forward past the suspension springs and contacted the more rigid seat pan frame. Either phenomenon would have applied a reaction force to the pelvis causing it to rotate rearward. Combined downward excursion and rearward rotation of the pelvis allowed for submarining of the HIII-5F. Submarining timing was evident in high-speed video and by sharp transitions in ASIS and lumbar load cell data. We hypothesise that submarining occurred first on the buckle side because there was no pre-tensioning on this side of the lap belt, allowing for more slack between the pelvis and lap-belt. Similar phenomena have been observed in computational studies, where the pelvis was more likely to disengage the lap belt on the buckle side in the absence of buckle pre-tensioning [7]. When the HIII-5F submarined and the belt slipped over the pelvis, it allowed for greater forward excursion of the pelvis compared to the other two tests (Figure 1).

Since the HIII-5F submarined in the only test performed without a SCAB, analysis of SCAB effects on forward pelvis excursion is limited to times prior to submarining occurrence. Comparisons made between the three tests performed for this study show that prior to submarining occurrence in restraint configuration #3, application of the SCAB reduced pelvis forward excursion (Fig. B7). This finding agrees with what has been observed in previous studies, both experimental [2, 27] and computational [22], that have shown a SCAB limits forward pelvis excursion.

Previous computational work has demonstrated that lap belt load is directly transferred to the lumbar spine when the lap belt loses engagement with the pelvis [7]. Consequently, at the time of submarining of the HIII-5F, left and right ASIS load cell forces were offloaded as force applied anteriorly to the lumbar spine increased (Figure 8). The positive anterior-posterior shear force combined with continued rearward rotation of the pelvis allowed the lumbar spine to better align with the direction of acceleration, increasing lumbar spine compression. Finally, increases in lumbar spine shear force and compression were coupled with increases in extension bending moment. When the pelvis reached peak forward excursion and the torso continued to flex forward prior to rebound, the lumbar spine was eventually put under tension and saw reductions in anterior-posterior shear force and extension bending moment.

While the increase in lumbar spine shear force amidst submarining agrees with what has been measured in previous computational work [7], the coinciding response of increased compression and extension bending moment after submarining contradicts lumbar spine responses recorded in previous studies. Previous research with PMHS and the Global Human Body Models Consortium (GHBMC) HBMs has suggested that lumbar spine compressive forces get offloaded when reclined occupants submarine [6, 22, 33]. The exact opposite trend was seen in this study, as the HIII-5F experienced the largest lumbar spine compressive forces when it submarined. This discrepancy might be explained by the use of a SCAB in this test series. It is possible that a SCAB reduces the maximum compression forces applied to the lumbar spine, and the notion that lumbar spine compressive forces get offloaded when reclined occupants submarine is a consequence of high lumbar spine compressive forces prior to submarining in current recline restraint environments. This discrepancy might also be explained by the different surrogates used to evaluate lumbar spine response and how and where lumbar spine response is measured across these surrogates. It is well known that the lumbar spine block of the Hybrid-III ATDs is not perfectly biofidelic [11, 28]. It is possible that the PMHS and GHBMC, which contain vertebrae, joints, ligaments, and most other anatomical structures of the lumbar spine, will measure different lumbar responses than the HIII-5F.

Effect of A P/T on Occupant Response

Large differences in HIII-5F kinematic and kinetic response were not observed when comparing the tests run in restraint configurations #1 and #2. The only difference between these restraint environments was that restraint configuration #2 included an A P/T while restraint configuration #1 did not. Although the test run without the A P/T had slightly higher shoulder belt forces, this did not have much, if any, impact on chest displacement (Fig. D10) nor chest acceleration. Head acceleration (Fig. D1-D3), chest displacement (Fig. D10), chest acceleration (Fig. D7-D9), upper neck forces (Fig. D13-D15), lumbar forces (Fig. 7-9), and femur forces (Fig. D11, Fig. D12) were similar across these two tests. Furthermore, both restraint configurations #1 and #2 led to similar responses at the head and neck.

Head and spine kinematics were similar across tests in configurations #1 and #2, while pelvis kinematics varied marginally. The test that included the A P/T promoted slightly better engagement of the lap belt with the HIII-5F pelvis. There was approximately 10 mm less forward excursion of the pelvis in restraint configuration #2 when compared to restraint configuration #1. Although the A P/T restricted initial upwards motion of the pelvis in restraint configuration #2, downwards displacement of the pelvis was similar across the two tests. There was approximately 2.5° less peak pelvis rearward rotation when the HIII-5F was tested in restraint configuration #2 with the A P/T. While reduced forward translation and rearward rotation are favorable pelvis kinematics, the cost was higher forces applied to the ASIS. There were approximately 410 N and 743 N more force applied to the left and right ASIS load cells, respectively, in restraint configuration #2 when compared to restraint configuration #1. Since higher ASIS forces may promote pelvis fracture [34], better protection might be offered to a human occupant in restraint configuration #1. Restraint configuration #1 was able to produce favorable pelvis kinematics and protect the HIII-5F from submarining while also minimising loads applied to the ASIS. Based solely on HIII-5F data in this test environment, the SCAB was the restraint that contributed the most to occupant protection because it was crucial in preventing the occupant from submarining. Alternatively, the A P/T was not critical for preventing submarining of the HIII-5F.

Novelty of Test Environment

The test environment in this study allowed us to evaluate occupant kinematics by incorporating vehicle structures and seat-integrated countermeasures. The HIII-5F was put in a non-traditional seated posture since the seatback was reclined 40° from the vertical, the HIII-5F feet were elevated off the floor, and the seat was positioned in the rearmost seat track position, which limited the ability of the knee bolster to help with pelvic restraint. Previous experimental setups for frontal impact testing of occupants in recline have focused on using simplified test environments for repeatability purposes, and as a result, have been unable to evaluate real-vehicle seats and seat-integrated restraints. Not only does the current study demonstrate that one seat-integrated countermeasure, the SCAB, might be critical in protecting small female occupants from submarining, it also sheds light on how a real-vehicle seat might influence pelvis downward displacement. In the absence of a SCAB, the HIII-5F pelvis had at least 62 mm of downward excursion into the seat. Unfortunately, since the pelvis marker clusters became obscured between 63-84 ms, we do not know the exact maximum downward displacement of the pelvis. Of the experimental frontal impact sled test studies performed on occupants in recline that reported H-point or pelvis downward displacement, Baudrit *et al.,* 2022 [15] reported less than 40 mm of downward pelvis displacement into the semi-rigid seat and Richardson *et al.,* 2020 [17] reported less than 20 mm of downward pelvis displacement into the semi-rigid seat. Both Baudrit *et al.,* 2022 and Richardson *et al.,* 2020 [15, 17] performed studies using mid-sized male PMHS. Of course, there are limitations to comparing these tests to the current study as the pulse, occupant size, occupant sex, surrogate type, and feet initial positions all varied. However, at a slightly higher pulse, with a surrogate of smaller mass, this study observed the HIII-5F experience almost double the maximum downward pelvis excursion that has been recorded previously for similar seated postures on the semi-rigid seat. Since downward displacement of the pelvis is such a critical factor in predicting submarining [6, 23], it makes sense that future studies focus on using real-vehicle seats to gain a more realistic understanding of downward pelvis excursion for different occupant sexes and sizes.

Limitations and Future Work

A limitation of this work is understanding whether the restraint effectiveness observed in our test environment with a HIII-5F can be translated to other occupant anthropometries. To understand whether the countermeasures that best protected the HII-5F will be the same for other occupants, future research should be conducted in similar test environments with other occupant anthropometries. Another limitation of this research is understanding whether the restraint effectiveness observed in our test environment with a HIII-5F can be translated to small-sized females. As was mentioned earlier, the lumbar spine biofidelity of the Hybrid-III ATDs is far from perfect [11, 28]. Lack of hip extension permitted by the HIII-5F may be another limitation of the HIII-5F's biofidelity. Furthermore, the submarining mechanism has been shown to differ between PMHS and the Hybrid-III ATD [11]. However, almost all biofidelity work related to the Hybrid-III ATD has been exclusively performed on the Hybrid-III 50th male (HIII-50M). To our knowledge, there is no study that has directly compared small-sized female kinematics and response between PMHS and the HIII-5F for frontal impacts, irrespective of the type of seat being used or the seated posture of the occupant. Future research should focus on making direct comparisons between the HIII-5F and other small-sized female surrogates. This research will provide critical data for comparison for other small-sized surrogates tested in similar environments.

V. CONCLUSION

While each restraint configuration tested in this study uniquely affected the kinematic and kinetic response of the HIII-5F, removal of the SCAB in restraint configuration #3 had the biggest impact on these measures. The HIII-5F submarined only in configuration #3, suggesting the SCAB played a substantial role in preventing submarining for configurations #1 and #2. The SCAB delayed and reduced pelvis downward excursion, which was effective in helping prevent submarining. When comparing configurations #1 and #2, the anchor pretensioner had some effect on pelvis kinematics and allowed for higher applied loads to the ASIS. Differences in injury metrics, such as head accelerations and angular rates, neck forces and moments, chest accelerations and displacements, and femur forces, did not suggest incorporating the anchor pretensioner provided benefit to protecting the HIII-5F in this test environment.

The test environment for this study allowed us to evaluate complete vehicle restraint configurations, equipped with seat-integrated restraints, for a HIII-5F seated in a reclined posture with legs elevated off the floor and the HIII-5F seated farther away from the IP than traditional mid-track seat position testing. To our knowledge, this study is the first frontal impact experimental study performed on a HIII-5F seated in a non-traditional posture, and the first frontal impact experimental study performed on any surrogate in a non-traditional posture seated in a real-vehicle seat. Not only does this research suggest that a SCAB might be critical in protecting small female occupants from submarining, but it also suggests that real-vehicle seats might allow for more maximum pelvis downward excursion than has been observed in simplified semi-rigid seats. Future research for occupants in alternative seating postures should focus on measuring occupant kinematics in real-vehicle seats and evaluating whether the restraint effectiveness provided to the HIII-5F in this study can be translated to small-sized female PMHS as well as surrogates of other anthropometries.

VI. ACKNOWLEDGEMENTS

We would like to acknowledge all those involved in the design, preparation, and execution of the sled tests at the University of Virginia's Center for Applied Biomechanics. We would also like to thank our sponsor, Hyundai Motor Company, for their support in this project.

VII. REFERENCES

[1] Jorlöv, S.; Bohman, K.; Larsson, A. (2017). Seating Positions and Activities in Highly Automated Cars – A Qualitative Study of Future Automated Driving Scenarios, *Proceedings of the International Research Conference on the Biomechanics of Impact*Presented at the IRCOBI, , Antwerp, Belgium, 13–22

[2] Östling, M.; Sunnevång, C.; Svensson, C.; Kock, H.-O. (2017). Potential future seating positions and the impact on injury risks in a Learning Intelligent Vehicle (LIV)Presented at the 11. VDI-Tagung Fahrzeugsicherheit, , Berlin, Germany

[3] Dissanaike, S.; Kaufman, R.; Mack, C. D.; Mock, C.; Bulger, E. (2008). The Effect of Reclined Seats on Mortality in Motor Vehicle Collisions, *Journal of Trauma and Acute Care Surgery*, Vol. 64, No. 3, 614. doi:10.1097/TA.0b013e318164d071

[4] McMurry, T. L.; Poplin, G. S.; Shaw, G.; Panzer, M. B. (2018). Crash safety concerns for out-of-position occupant postures: A look toward safety in highly automated vehicles, *Traffic Injury Prevention*, Vol. 19, No. 6, 582–587. doi:10.1080/15389588.2018.1458306

[5] Schaefer, L. C.; Junge, M.; Vörös, I.; Koçaslan, K.; Becker, U. (2021). Odds ratios for reclined seating positions in real-world crashes, *Accident Analysis & Prevention*, Vol. 161, 106357. doi:10.1016/j.aap.2021.106357

[6] Boyle, K. J.; Reed, M. P.; Zaseck, L. W.; Hu, J. (2019). A Human Modelling Study on Occupant Kinematics in Highly Reclined Seats during Frontal Crashes, *Proceedings of the International Research Conference on the Biomechanics of Impact*Presented at the ICROBI, , Florence, Italy, 282–292

[7] Gepner, B.; Rawska, K.; Richardson, R.; Kulkarni, S.; Chastain, K.; Zhu, J.; Forman, J.; Kerrigan, J. (2019). Challenges for Occupant Safety in Highly Automated Vehicles Across Various Anthropometries, *26th International Technical Conference on the Enhanced Safety of Vehicles (ESV): Technology: Enabling a Safer TomorrowNational Highway Traffic Safety Administration*Presented at the ESV

[8] Lin, H.; Gepner, B.; Wu, T.; Forman, J.; Panzer, M. (2018). Effect of Seatback Recline on Occupant Model Response in Frontal CrashesPresented at the IRCOBI, , Athens, Greece, 386–387

[9] Rawska, K.; Gepner, B.; Kulkarni, S.; Chastain, K.; Zhu, J.; Richardson, R.; Perez-Rapela, D.; Forman, J.; Kerrigan, J. R. (2019). Submarining sensitivity across varied anthropometry in an autonomous driving system environment, *Traffic Injury Prevention*, Vol. 20, No. sup2, S123–S127. doi:10.1080/15389588.2019.1655734

[10] Adomeit, D.; Heger, A. (1975). Motion Sequence Criteria and Design Proposals for Restraint Devices in Order to Avoid Unfavorable Biomechanic Conditions and Submarining, *SAE Transactions*, Vol. 84, 3150–3159

[11] Luet, C.; Trosseille, X.; Drazétic, P.; Potier, P.; Vallancien, G. (2012). Kinematics and Dynamics of the Pelvis in the Process of Submarining using PMHS Sled Tests, *Stapp Car Crash Journal*, Vol. 56. doi:10.4271/2012-22-0011

[12] Patrick, L. M.; Levine, R. S. (1975). *Injury to Unembalmed Belted Cadavers in Simulated Collisions* (SAE Technical Paper 751144)Warrendale, PA, SAE International. doi:10.4271/751144

[13] Richardson, R.; Jayathirtha, M.; Donlon, J. P.; Forman, J. L.; Gepner, B.; Östling, M.; Mroz, K.; Pipkorn, B.; Kerrigan, J. R. (2020). Pelvis Kinematics and Injuries of Reclined Occupants in Frontal Impacts, *Proceedings of the International Research Conference on the Biomechanics of Impact*Presented at the IRCOBI, , 499–515

[14] Shin, J.; Donlon, J. P.; Richardson, R.; Espelien, C.; Gallaher, M.; Luong, V.; Gepner, B.; Forman, J.; Östling, M.; Kerrigan, J. (2023). Comparison of Pelvis Kinematics and Injuries in Reclined Frontal Impact Sled Tests Between Mid-Size Adult Male and Female PMHS, *Proceedings of the International Research Conference on the Biomechanics of Impact*Presented at the IRCOBI, , Cambridge, United Kingdom, 266–284

[15] Baudrit, P.; Uriot, J.; Richard, O.; Debray, M. (2022). Investigation of Potential Injury Patterns and Occupant Kinematics in Frontal Impact with PMHS in Reclined Postures, *STAPP CAR CRASH JOURNAL 2022 Volume 66*, Vol. 66, No. 1. doi:10.4271/2022-22-0001

[16] Östling, M.; Lundgren, C.; Nils, L.; Huf, A.; Wernicke, P.; Pipkorn, B. (2021). The Influence of a Seat Track Load Limiter on Lumbar Spine Compression Forces in Relaxed, Reclined, and Upright Seating Positions: A Sled Test Study using THOR-50M, *Proceedings of the International Research Conference on the Biomechanics of Impact*Presented at the IRCOBI, , 361–379

[17] Richardson, R.; Donlon, J.-P.; Jayathirtha, M.; Forman, J. L.; Shaw, G.; Gepner, B.; Kerrigan, J. R.; Östling, M.; Mroz, K.; Pipkorn, B. (2020). Kinematic and Injury Response of Reclined PMHS in Frontal Impacts, *Stapp Car Crash Journal*, Vol. 64. doi:10.4271/2020-22-0004

[18] Richardson, R.; Donlon, J.; Chastain, K.; Shaw, G.; Forman, J.; Sochor, S.; Jayathirtha, M.; Kopp, K.; Overby, B.; Gepner, B.; Kerrigan, J.; Östling, M.; Mroz, K.; Pipkorn, B. (2019). Test Methodology for Evaluating the Reclined Seating Environment with Human Surrogates, *Proceedings of the 26th International Technical Conference on the Enhanced Safety of Vehicles*Presented at the ESV, , Eindhoven, Netherlands

[19] Shin, J.; Donlon, J. P.; Richardson, R.; Gepner, B.; Forman, J.; Östling, M.; Kerrigan, J. (2022). Biofidelity Evaluation of the Hybrid-III 50th Male and the THOR-50M in Reclined Frontal Impact Sled Tests, *Proceedings of the International Research Conference on the Biomechanics of Impact*Presented at the IRCOBI, , Porto, Portugal, 309–331

[20] Somasundaram, K.; Hauschild, H.; Driesslein, K.; Pintar, F.; Richardson, R.; Parent, D. (2023). THOR-05F biofidelity evaluation in reclined and upright seated postures subjected to frontal crash pulses, *Accident Analysis & Prevention*, Vol. 191, 107185. doi:10.1016/j.aap.2023.107185

[21] Somasundaram, K.; Hauschild, H.; Driesslein, K.; Pintar, F. A. (2024). Small Female Occupant Response in Reclined and Upright Seated Postures in Frontal Impacts, *Journal of Biomechanical Engineering*, Vol. 146, No. 031002. doi:10.1115/1.4062708

[22] Rawska, K.; Gepner, B.; Kerrigan, J. R. (2021). Effect of various restraint configurations on submarining occurrence across varied seat configurations in autonomous driving system environment, *Traffic Injury Prevention*, Vol. 22, No. sup1, S128–S133. doi:10.1080/15389588.2021.1939872

[23] Tang, L.; Zheng, J.; Zhou, Q. (2020). Investigation of risk factors affecting injuries in reclining seat under frontal impact, *International Journal of Vehicle Safety*, Vol. 11, No. 3, 247–274. doi:10.1504/IJVS.2020.109277

[24] Matsushita, T.; Saito, H.; Sunnevång, C.; Östling, M.; Vishwanatha, A.; Tabhane, A. (2019). Evaluation of the Protective Performance of a Novel Restraint System for Highly Automated Vehicles (HAV)Presented at the 26th International Technical Conference on the Enhanced Safety of Vehicles (ESV): Technology: Enabling a Safer TomorrowNational Highway Traffic Safety Administration

[25] Rashidy, M.; Deshpande, B.; T.j, G.; Morris, R.; Munson, R. A.; Lindberg, J. A.; Summers, L. (2001). Analytical Evaluation of an Advanced Integrated Safety Seat Design in Frontal, Rear, Side, and Rollover CrashesPresented at the International Technical Conference on Enhanced Safety of Vehicles

[26] Forman, J.; Lin, H.; Gepner, B.; Wu, T.; panzer, M. (2019). Occupant Safety in Automated Vehicles, *International Journal of Automotive Engineering*, Vol. 10, No. 2, 139–143. doi:10.20485/jsaeijae.10.2_139

[27] Shaw, G.; Lessley, D.; Ash, J.; Acosta, S.; Heltzel, S.; Riley, P.; Kim, T.; Crandall, J. (2018). Pelvic restraint cushion sled test evaluation of pelvic forward motion, *Traffic Injury Prevention*, Vol. 19, No. 3, 250–255. doi:10.1080/15389588.2017.1326106

[28] Baudrit, P.; Potier, P.; Petit, P.; Trosseille, X.; Vallancien, G. (2005). CADAVER AND DUMMY INVESTIGATION OF INJURY RISK WITH ANTI-SLIDING SYSTEM IN CASE OF STATIC DEPLOYMENT, *19th International Technical Conference on the Enhanced Safety of Vehicles*Presented at the ESV, , 6–9

[29] J211/1_202208: Instrumentation for Impact Test, Part 1 - Electronic Instrumentation - SAE International. (n.d.), from https://www.sae.org/standards/content/j211/1_202208/, accessed 21-4-2025

[30] Parts List and Drawings Part 572 Subpart O Hybrid III 5th Percentile Small Adult Female Crash Test Dummy (H-III5F Alpha Version). (2002, June), Office of Crashworthiness Standards and Vehicle Research and Test Center National Highway Traffic Safety Administration

[31] 880105-9900 User Manual Hybrid III 5th Female Rev G. (2020), Humanetics

[32] Shaw, G.; Parent, D.; Purtsezov, S.; Lessley, D.; Crandall, J.; Kent, R.; Guillemot, H.; Ridella, S. A.; Takhounts, E.; Martin, P. (2009). Impact Response of Restrained PMHS in Frontal Sled Tests: Skeletal Deformation Patterns Under Seat Belt Loading, *Stapp Car Crash Journal*, Vol. 53. doi:10.4271/2009-22-0001

[33] Richardson, R.; Jayathirtha, M.; Chastain, K.; Donlon, J.-P.; Forman, J.; Gepner, B.; Östling, M.; Mroz, K.; Shaw, G.; Pipkorn, B.; Kerrigan, J. (2020). Thoracolumbar spine kinematics and injuries in frontal impacts with reclined occupants, *Traffic Injury Prevention*, Vol. 21, No. sup1, S66–S71. doi:10.1080/15389588.2020.1837365

[34] Moreau, D.; Chernyavskiy, P.; Sochor, S.; Gepner, B.; Forman, J.; Östling, M.; Kerrigan, J. R. (2023). Development of an Injury Risk Function for the Anterior Pelvis Under Frontal Lap Belt Loading Conditions, *Annals of Biomedical Engineering*, Vol. 51, No. 9, 1942–1949. doi:10.1007/s10439-023-03244-8

VIII. APPENDIX

Appendix A – Test Environment Setup

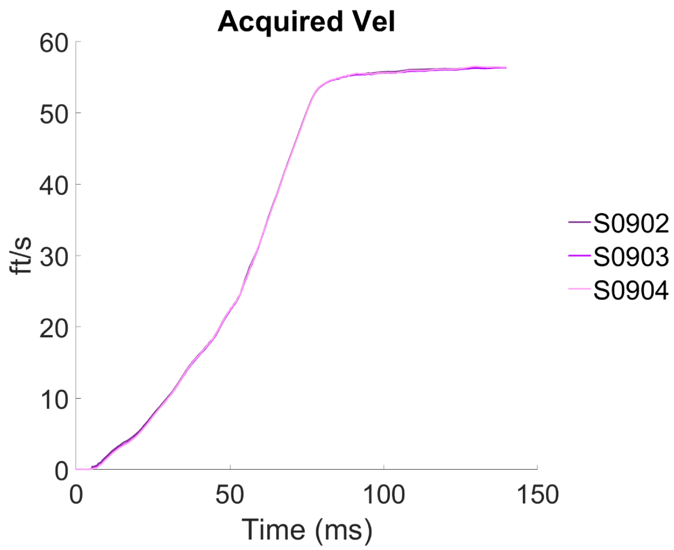

Fig. A1. The 56 km/h sled pulse used for the three sled tests in this study.

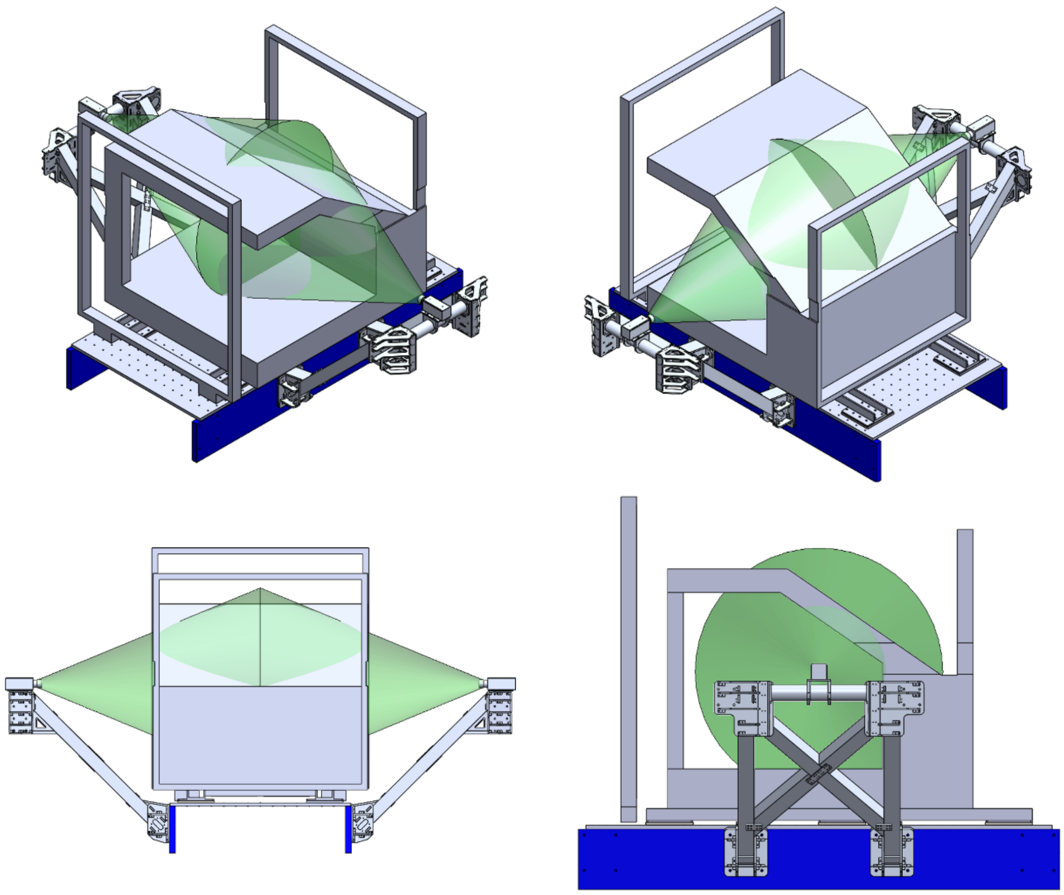

Fig. A2. CAD sketches of the outriggers mounted to the side of the SESA sled along with the outrigger and camera positions relative to the buck.

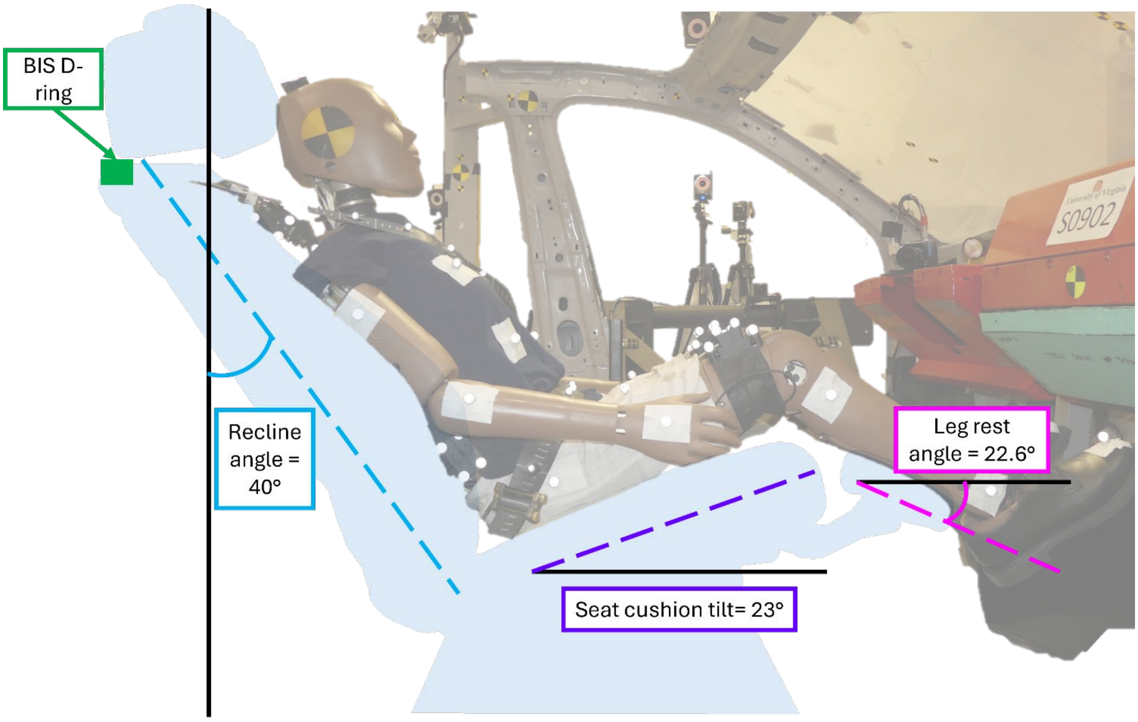

Fig. A3. Seat initial positioning targets.

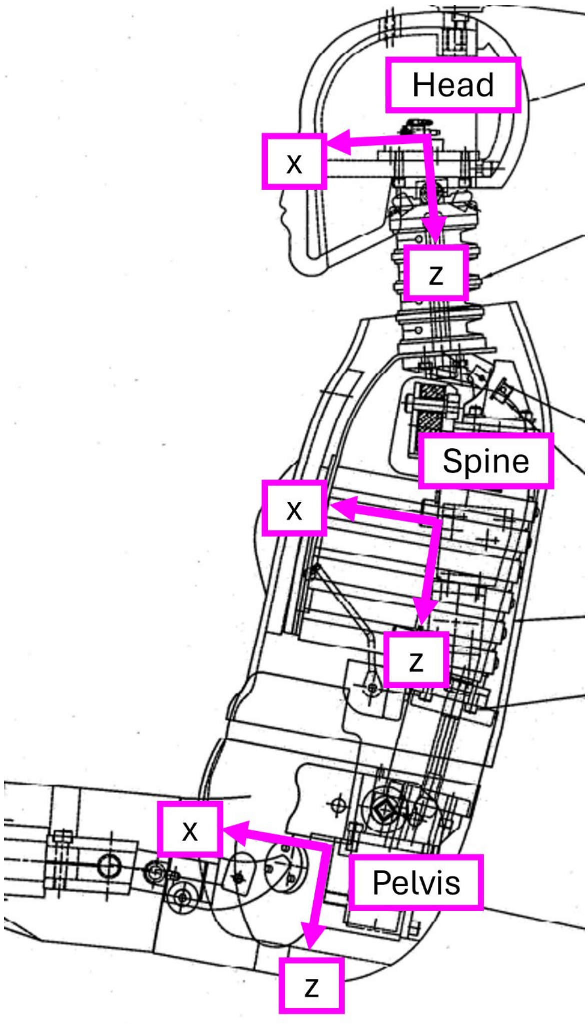

Fig. A4. Local anatomical structure CS for the HIII-5F. A more detailed description can be found in Appendix A of Shin et al. 2022. The coordinate system definitions of the HIII-5F were adapted from those used for the HIII-50M.

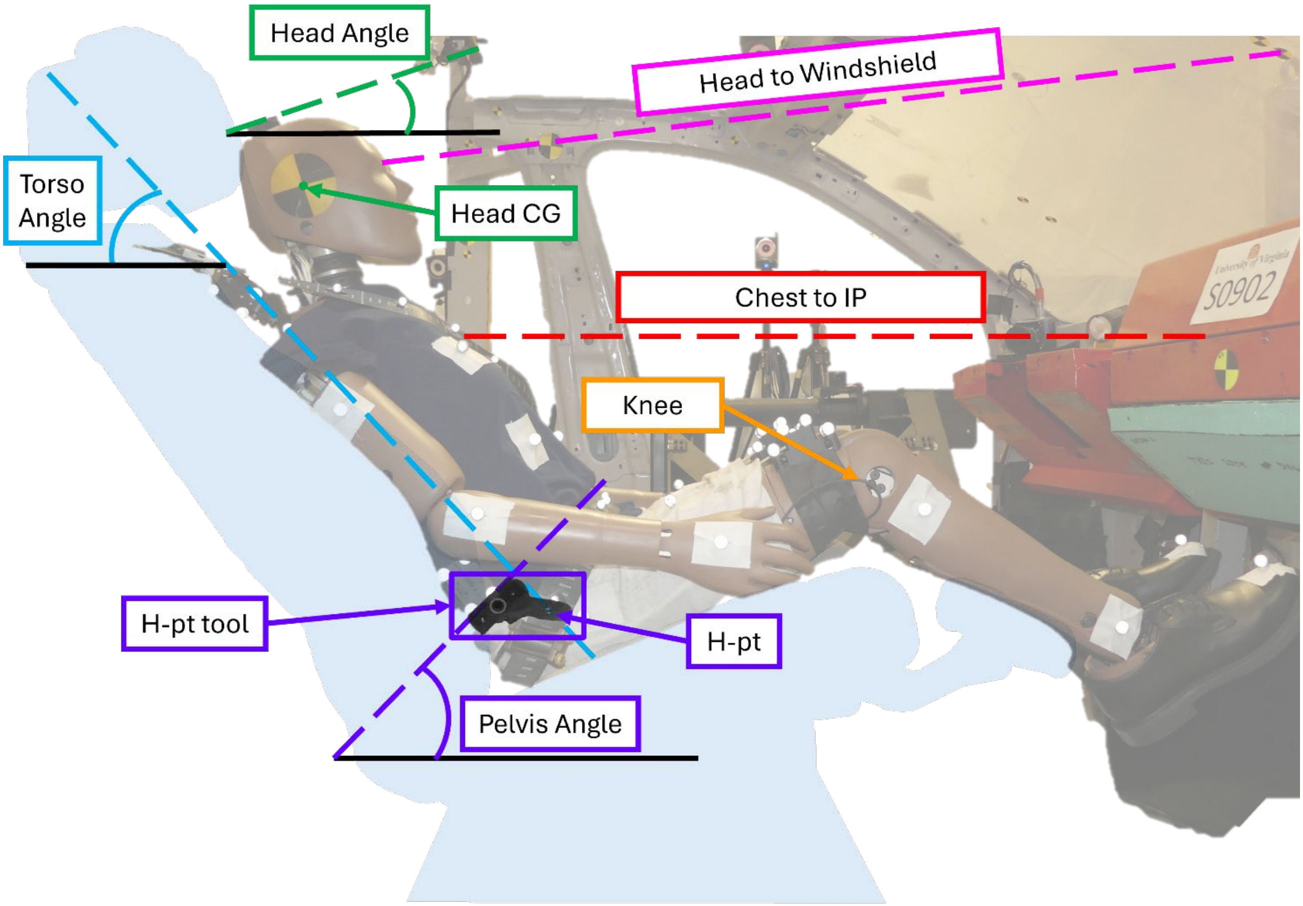

Fig. A5. HIII-5F initial positioning targets.

Appendix B – Kinematics

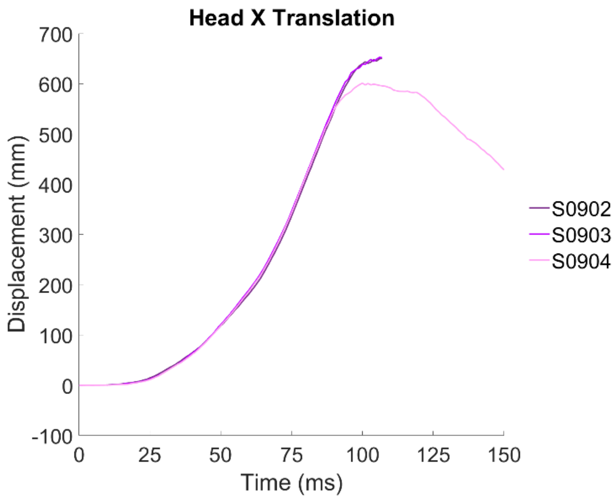

Fig B1. Head x-displacement time history relative to the global CS. Positive displacement corresponds with forward excursion of the head. For S0902 and S0903, VICON visibility of the head marker cluster was lost at 108 ms.

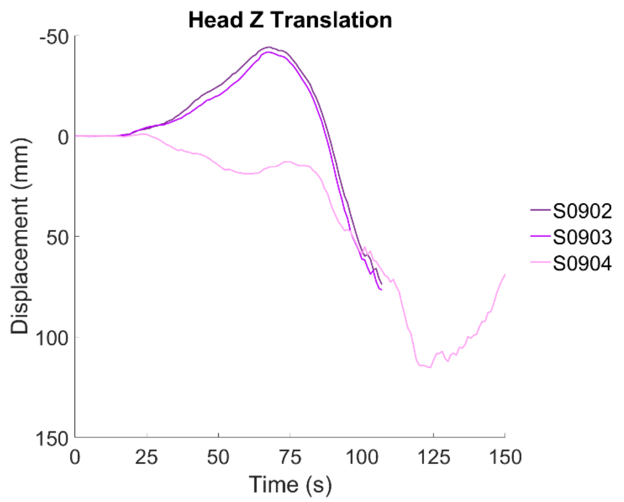

Fig B2. Head z-displacement time history relative to the global CS. Negative displacement corresponds with upwards excursion of the head. For S0902 and S0903, VICON visibility of the head marker cluster was lost at 108 ms.

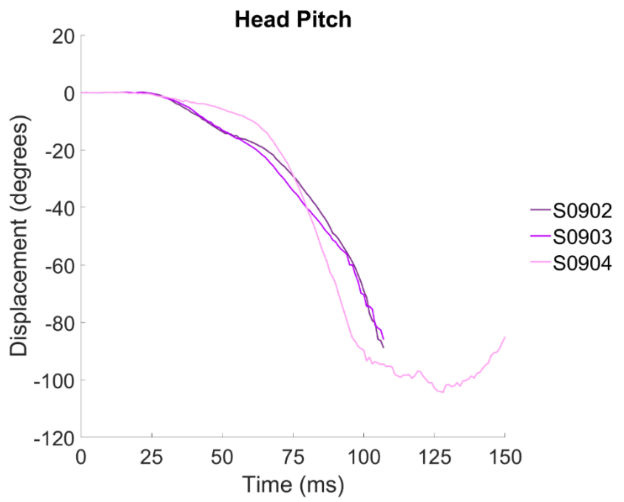

Fig. B3. Head rotation in the sagittal plane relative to the global CS. Negative displacement corresponds with forward rotation of the head. For S0902 and S0903, VICON visibility of the head marker cluster was lost at 108 ms.

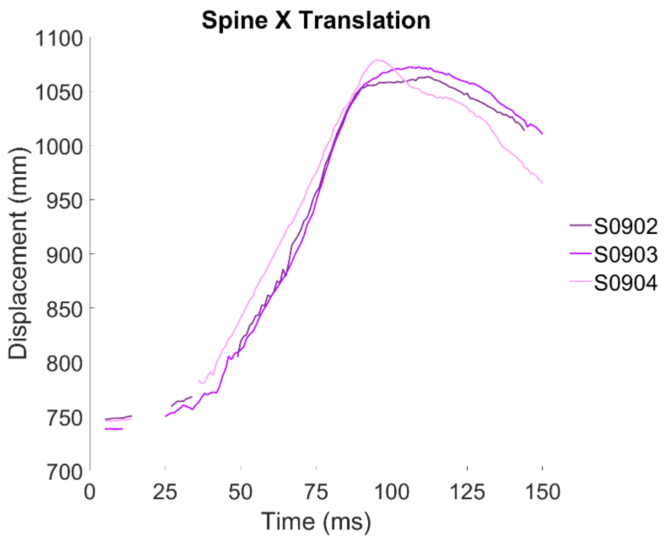

Fig B4. Spine x-displacement time history relative to the global CS. Positive displacement corresponds with forward excursion of the spine.

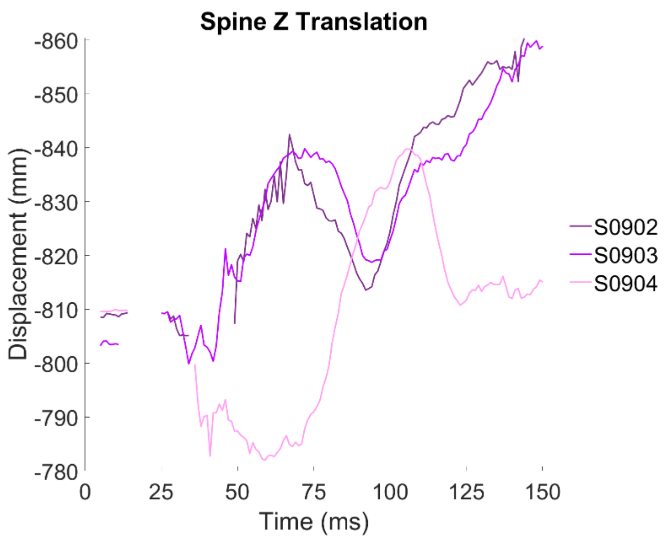

Fig B5. Spine z-displacement time history relative to the global CS. Negative displacement corresponds with upwards excursion of the spine.

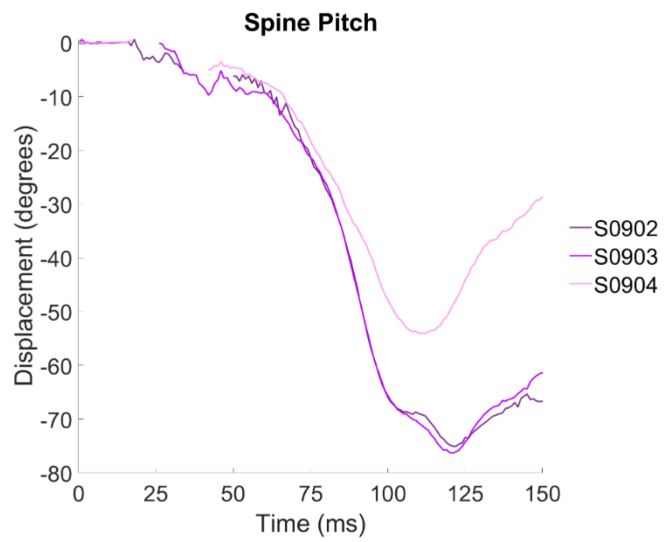

Fig. B6. Spine rotation in the sagittal plane relative to the global CS. Negative displacement corresponds with forward rotation (flexion) of the spine.

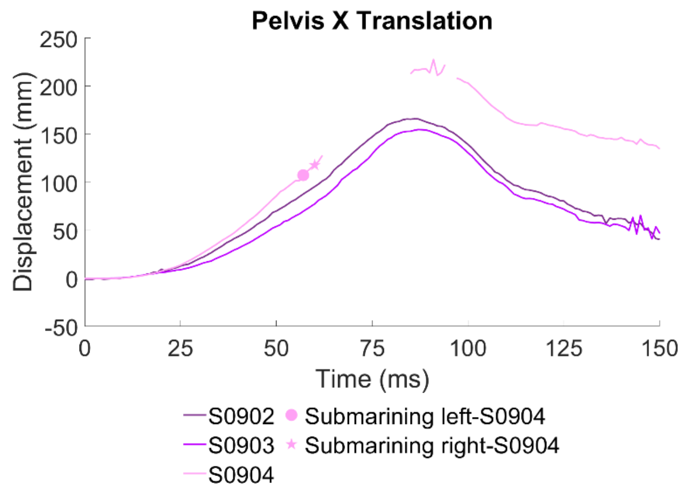

Fig B7. Pelvis x-displacement time history relative to the global CS. Positive displacement corresponds with forward excursion of the pelvis. Submarining in S0904 is marked on the pelvis trajectory. Submarining on the buckle-side is denoted by a circle. Submarining on the anchor side is denoted by a star. After submarining, between 63-84 ms, VICON visibility of the pelvis marker clusters was lost.

Appendix C – Belt Performance

TABLE CI BELT PERFORMANCE MEASUREMENTS			
	S0902	**S0903**	**S0904**
Webbing Length in shoulder retractor prior to each test [cm]	130.5	116.5	115.5
Pay-in	80	100	100
Pay-out	220	210	270

Appendix D – Sensor Data

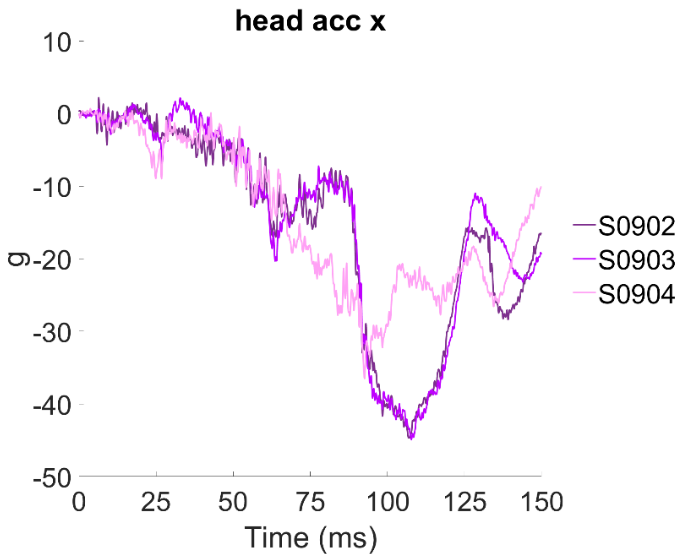

Fig. D1. Head acceleration along the x-axis. Filtered with a cfc1000 filter.

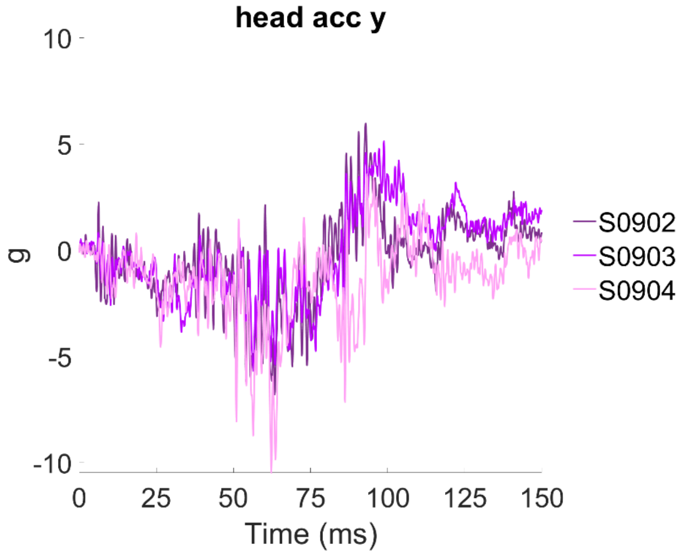

Fig. D2. Head acceleration along the y-axis. Filtered with a cfc1000 filter.

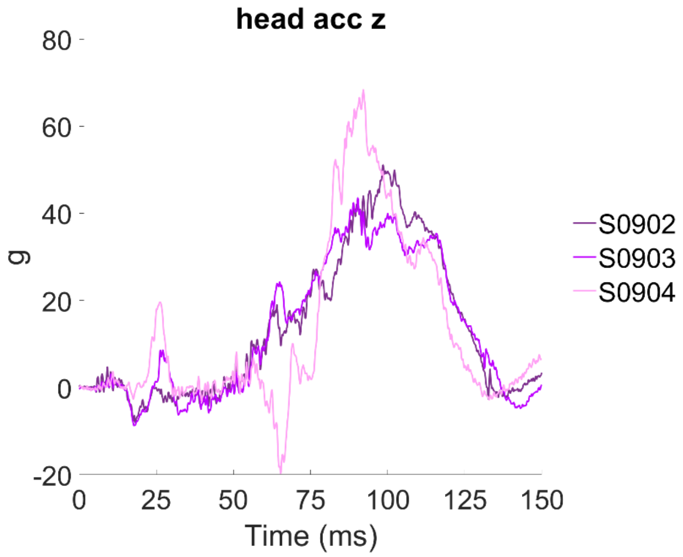

Fig. D3. Head acceleration along the z-axis. Filtered with a cfc1000 filter.

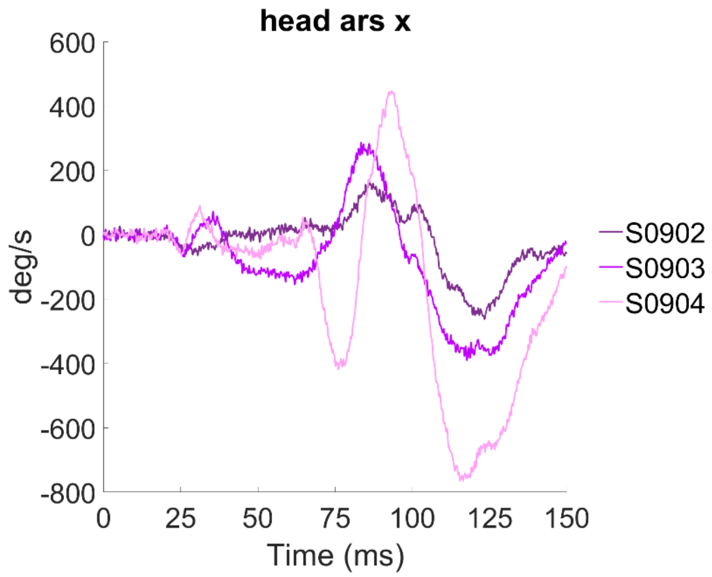

Fig. D4. Head angular rate about the x-axis. Filtered with a cfc1000 filter.

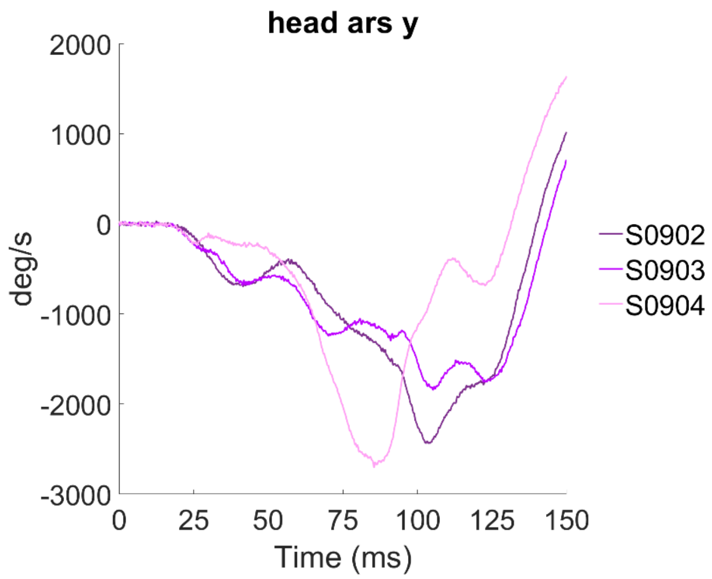

Fig. D5. Head angular rate about the y-axis. Filtered with a cfc1000 filter.

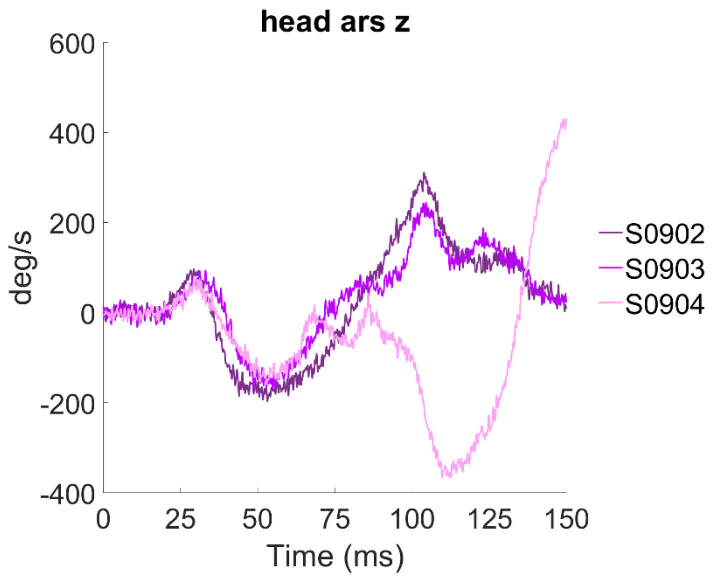

Fig. D6. Head angular rate about the z-axis. Filtered with a cfc1000 filter.

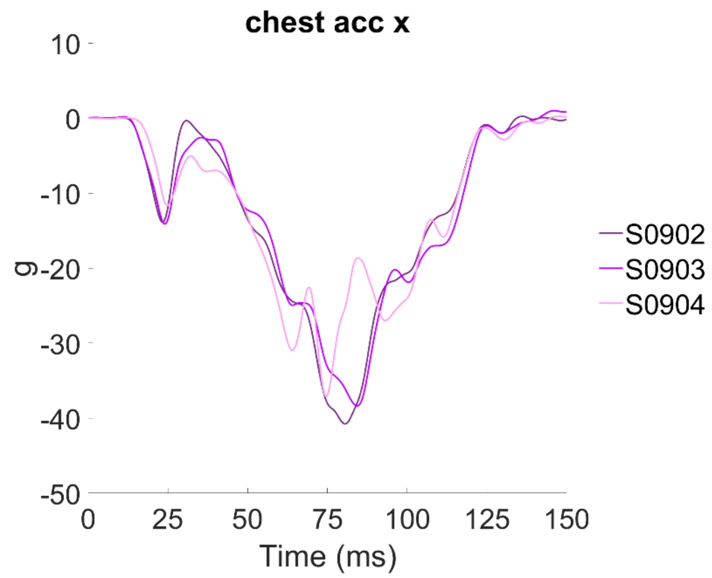

Fig. D7. Chest acceleration along the x-axis. Filtered with a cfc60 filter.

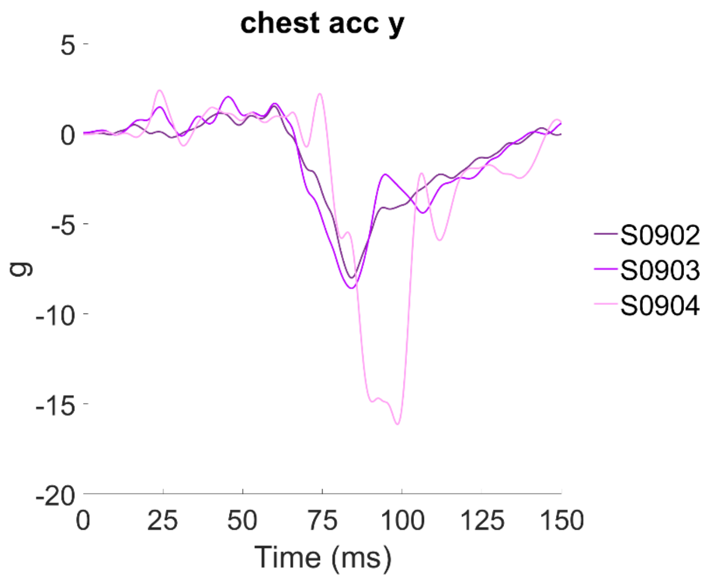

Fig. D8. Chest acceleration along the y-axis. Filtered with a cfc60 filter.

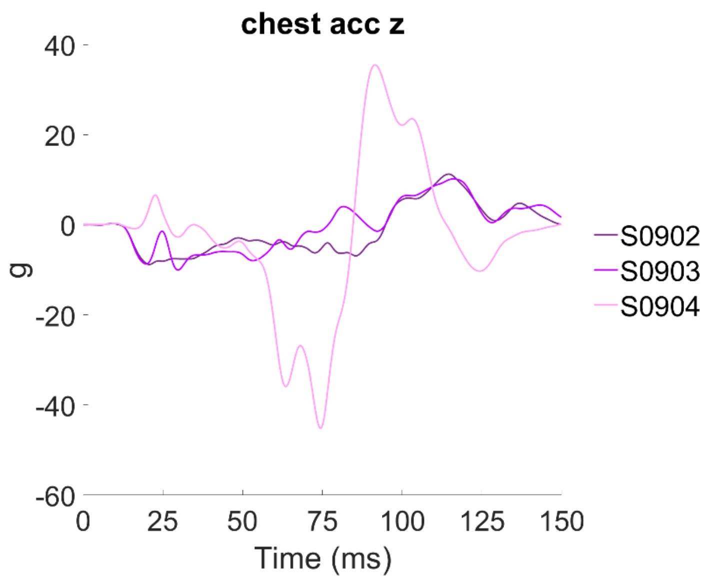

Fig. D9. Chest acceleration along the z-axis. Filtered with a cfc60 filter.

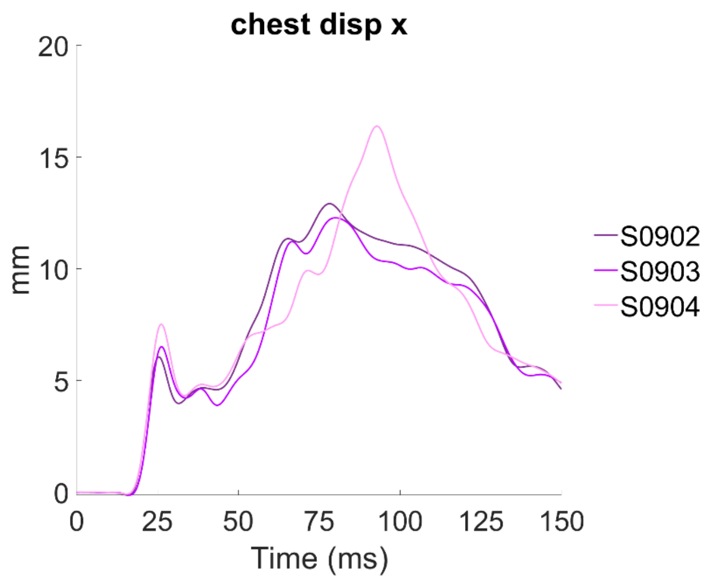

Fig. D10. HIII-5F chest displacement.

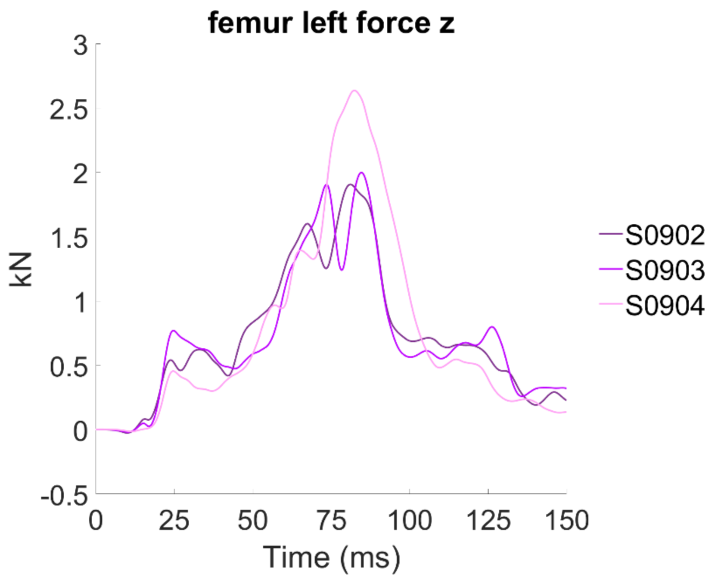

Fig. D11. Left femur force. Tension is positive. Compression is negative.

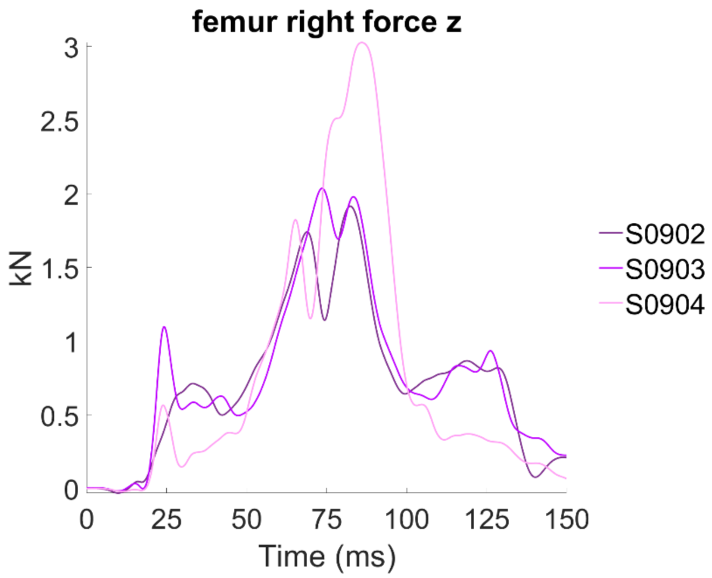

Fig. D12. Right femur force. Tension is positive. Compression is negative.

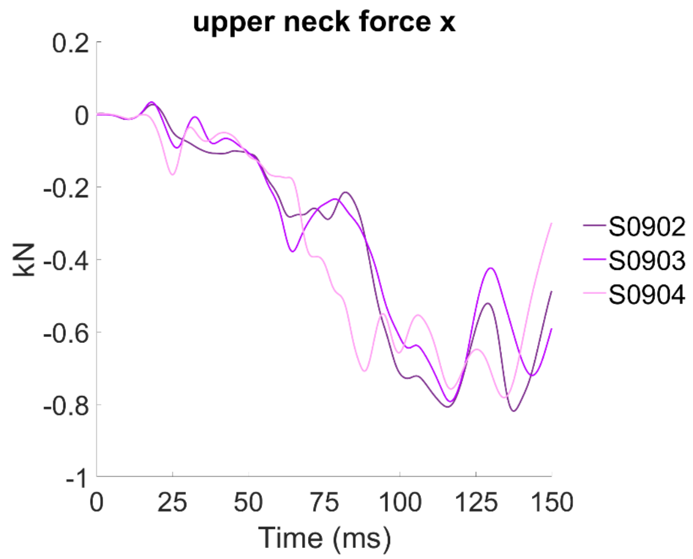

Fig. D13. Upper neck anterior-posterior shear force. Positive forces can be described by rearward motion of the head and forward motion of the chest.

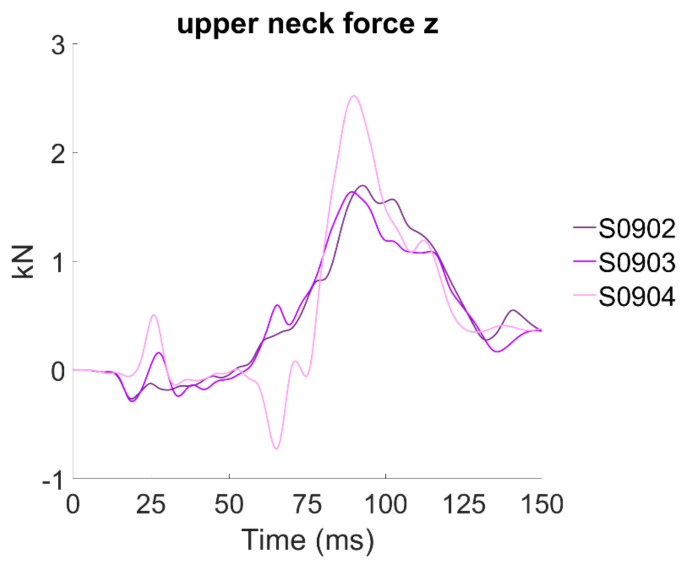

Fig. D14. Upper neck axial loads. Compression is negative. Tension is positive.

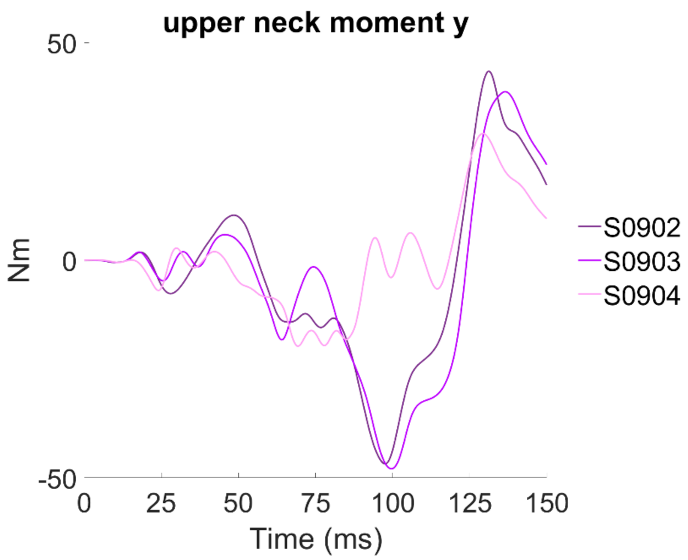

Fig. D15. Upper neck flexion-extension bending moment. Flexion bending moment is positive (chin rotating towards sternum). Extension bending moment is negative (chin rotating away from sternum).

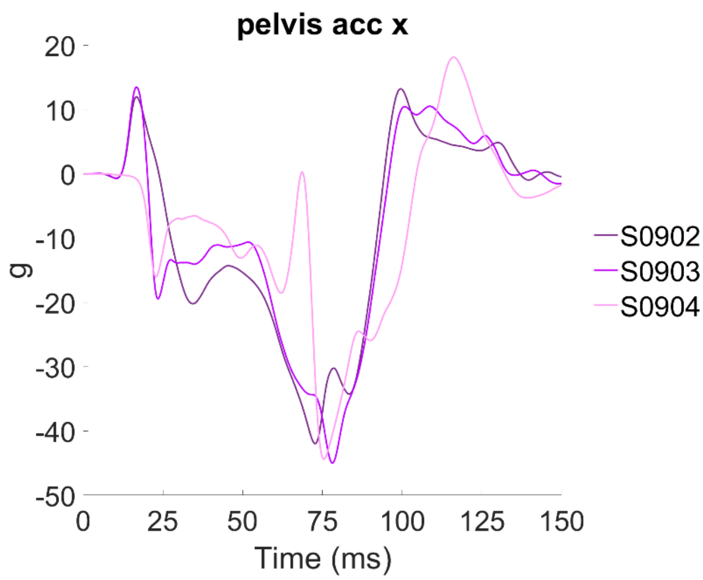

Fig. D16. Pelvis acceleration along the x-axis. Filtered with a cfc60 filter.

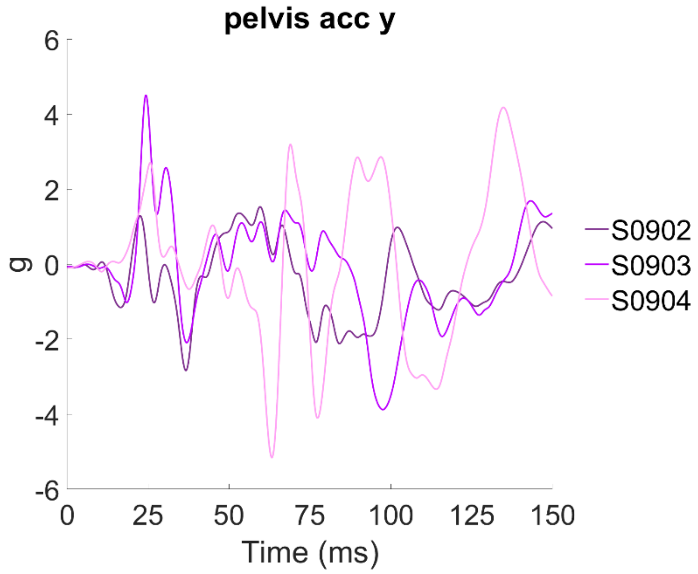

Fig. D17. Pelvis acceleration along the y-axis. Filtered with a cfc60 filter.

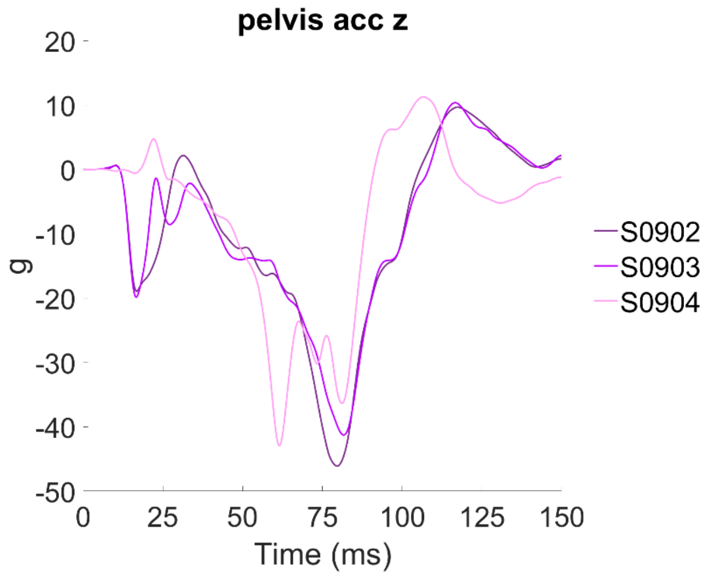

Fig. D18. Pelvis acceleration along the z-axis. Filtered with a cfc60 filter.